MODELLING OF CARBON BEHAVIOUR IN THE EDGE PLASMA OF RFX

F. Sattin[1], L. Carraro, M.E. Puiatti, R. Pugno[1,2], P. Scarin and M. Valisa

Consorzio RFX, corso Stati Uniti 4, 35127 Padova, Italy
[1]*INFM, Unità di Padova, corso Stati Uniti 4, 35127 Padova, Italy*
[2]*Dipartimento di Ingegneria Elettrica, Università di Padova, Italy*

In this work we illustrate some details of a 3D Monte Carlo code designed for the study of the impurities carbon and helium at the edge region of RFX. As a first selected application we present a parametric study of the screening of atomic carbon injected from the wall in dependence of various experimental situations.

1. The structure of the code

The code it is patterned after the LIM code [1] with some differences due to the peculiarity of the machine (e.g. the magnetic field shear, the absence of limiters and divertors and the presence of strong plasma deformations) A number N of particles is injected from the wall into the plasma. Each particle is followed along its trajectory until it strikes back the wall or enters the main plasma. The motion is divided into temporal steps of duration dt. A spatial distribution function is generated by recording the amount of time T_i that the i-th particle of charge Q spends at each spatial location. The main steps that each particle undergoes are:

1. The particle enters the edge plasma from a given location of the wall and with a given velocity **v**. In the particular simulation here presented only carbon atoms are injected, even though methane and helium may be studied as well. The particles are supposed to enter from the equatorial plane with radial inward direction.

2. The environment into which the particle moves is given from the beginning: the profiles of electron temperature and density, of magnetic field and radial electric field, of neutrals and of protons, and the plasma velocity of rotation are already known. The background is considered as unaffected by the presence of the impurities.

3. At each time step the particle can be ionized due to an electron collision with probability $P = 1 - \exp(-dt\ \upsilon)$. The frequencies υ are taken from [2].

4. Prior to ionization the particle follows a straight line. After the ionization, one must solve the Newton's equation

$$\mathbf{F} = m\mathbf{a} = Ze(\mathbf{E} + \mathbf{v} \times \mathbf{B}) + \frac{\mathbf{V}_B - \mathbf{v}}{\tau_{frict}} \qquad (1)$$

The last term is the viscous force, which derives from the friction between the particle and the background plasma. τ_{frict} is the time of equipartition of momentum [1]. $\mathbf{V}_B$ is the collective velocity of the plasma. **E** and **B** are the macroscopic electric and magnetic fields in the plasma. The Lorentz force **v** x **B** is usually not retained in similar codes, since this term gives rise to a Larmor gyration with a radius ρ_L which is usually negligible with respect to all length scales in Tokamaks. The motion of the particle is instead replaced by the motion of its guiding centre, adding to Eq. (1) the drift forces. In Reversed Field Pinches B is smaller by an order of magnitude than in Tokamaks, therefore effects related to the finite Larmor radius (which is of the order of 1 mm or more) may be in principle not negligible. The effect of the several Coulomb microcollisions suffered by the particle are simulated adding a diffusion term to the spatial displacement: $dx \rightarrow dx + R\sqrt{2Ddt}$, where R is a random number uniformly chosen in the interval (-1,1) and D is a diffusion coefficient. Cross-field diffusion $D_\perp$ has been considered as an anomalous process, its value is given accordingly with the estimates given by independent models (e.g. fluid models [3]). For diffusion along magnetic field lines, the Spitzer expression has been adopted. In the velocity space the interaction with the plasma results in a thermalization of the particle. The time step is automatically adjusted by the code so that the maximum elongation be small (0.1 mm) compared with all length scales. This may turn into very short *dt*'s.

5. The particle may end its travel entering the core plasma or returning to the wall. In this latter case the calculation is stopped and the position and velocity of arrival are recorded to be used for the next generation of particles.

6. Once all the particles have finished their run, a second generation can be created to take into account the self-sputtering process. At each wall location where a particle is lost, another one is generated with a probability given by the yields found in literature [4]. The trajectories of these second-generation particles are followed in the same terms as the former ones.

2. Selected applications

The code has been until now mostly used in a 2D geometry, assuming symmetry along the toroidal direction. In this section we show some selected applications. We focus here on the important topic of the screening. We have done a parametric study by varying all major parameters (temperature, density, magnetic field, diffusion). Self sputtering was neglected. We studied: penetration length in radial direction and parallel to the wall; screening efficiency. Let us recall that geometric parameters of RFX are: major radius R = 2m, minor radius a = 0.46m. The reference plasma parameters are those of a medium current (600 kA) RFX shot: $T_e(0)$ = 200 eV; $T_e(a)$ = 15 eV; $n_e(0) = 4 \cdot 10^{19}$ m^{-3}; $n_e(a) = 3 \cdot 10^{18}$ m^{-3}; $B_{pol}(a)$ = 0.3 T; Z_{eff} = 2. The plasma column is rigidly shifted in the horizontal direction outwards by 1 cm. In RFX temperature and density profiles are steep functions of the minor radius, usually

approximated with a power law: $1-(r/a)^{\alpha}$, with α around 4 for T_e and 30 for n_e. Impurity cross field diffusion is known to vary around 10 m^2/s [3]. The entrance velocity of reference for injected particles is 4 km/s, corresponding to a kinetic energy of 1 eV per atom. The studies were performed by varying: a) $B_{pol}(a)$; b) The diffusion; c) The electron temperature; d) The electron density; e) The entrance energy.

In Figure 1 we show the radial profiles of CI, CII and CIII on the equatorial plane for various conditions. The main features to be remarked are listed in Table 1 and are: a) the ionization length of CI varies in the range 0.4 - 1.3 cm and in standard condition is 0.7 cm. All this is in quite a good accordance with simple analytical estimates. λ_{ion}(CI) recovered by the simulation is unaffected by parameters other than the entrance velocity or temperature and density profiles. b) CII and CIII profiles are instead sensitive also to **B** and, to a larger extent, to diffusion.

The profile of redeposition revealed no marked trend in dependence of any of the parameters, its width being always around 10-15 cm (but the finest resolution used was of about 5 cm). We do expect the poloidal profile to be dominated by parallel diffusion, therefore only a dependence on temperature and density is expected, and is actually found.

With the term screening efficiency Σ we mean the fraction of particles injected which return to the wall without entering into the main plasma. A summary of the results for Σ is listed in Table 1. Some remarkable results can be recovered. In all cases the total screening is rather high, raising up even beyond 90%. The interest of the study was to understand which mechanism is the main responsible for the screening. The screening efficiency is dependent upon magnetic field, even though beyond what expected from an estimate using only the finite Larmor radius of the impurities as loss mechanism to the wall. It is a strongly decreasing function of the entrance velocity and shows a weaker dependence from T_e and/or n_e and an even weaker dependence from D.

3. Conclusions

The present results suggest that RFX has a large screening of the impurities coming from the wall, and that this effect is mainly due to the combined action of very steep gradients of temperature and density, together with a non-negligible radial diffusion.

References

[1] P.C. Stangeby, C. Farrell, S. Hoskins: L. Wood, Nucl. Fus. **28** (1988) 1945.

[2] K.L. Bell et al.: J. Phys. Chem. Ref. Data **12** (1983) 891.

[3] L. Carraro et al.: Nucl. Fus. **36** (1996) 1623.

[4] W. Eckstein, J. Bohdansky, J. Roth: Suppl. Nucl. Fus. **1** (1991) 51; W. Eckstein: J. Nucl. Mat. **248** (1997) 1; J. Roth, C. García-Gonzales: Nucl. Fus. **36** (1996) 1647.

#run	Note	Σ (%)	λ_{ion} CI [cm]
1	reference conditions	86	0.7
2	B=0.8T	85	0.7
3	B=0.5T	84	0.7
4	B=0.1T	78	0.7
5	$n_e(r=a)=1\ 10^{18}m^{-3}$	69	1.3
6	$n_e(r=a)=9\ 10^{18}m^{-3}$	90	0.4
7	$n_e(r=a)=1.2\ 10^{19}m^{-3}$	91	0.4
8	$T_e(r=a)=45eV$	92	0.4
9	$T_e(r=a)=60eV$	93	0.4
10	$D=1m^2/s$	87	0.7
11	$D=100m^2/s$	83	0.7
12	Esputtering=10eV	69	1.3
13	Esputtering=0.25eV	90	0.4

Table 1. Screening efficiency (column 2) and radial ionization length of CI (column 3). References conditions (first row) are outlined in the text. All other runs have been done by varying just one parameter at a time.

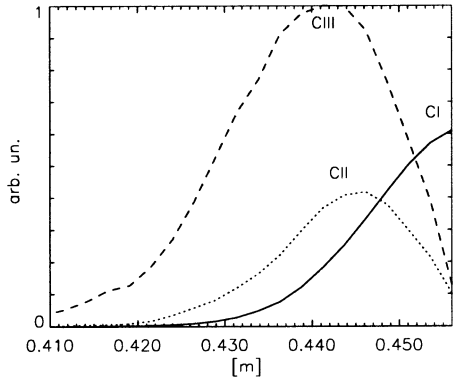

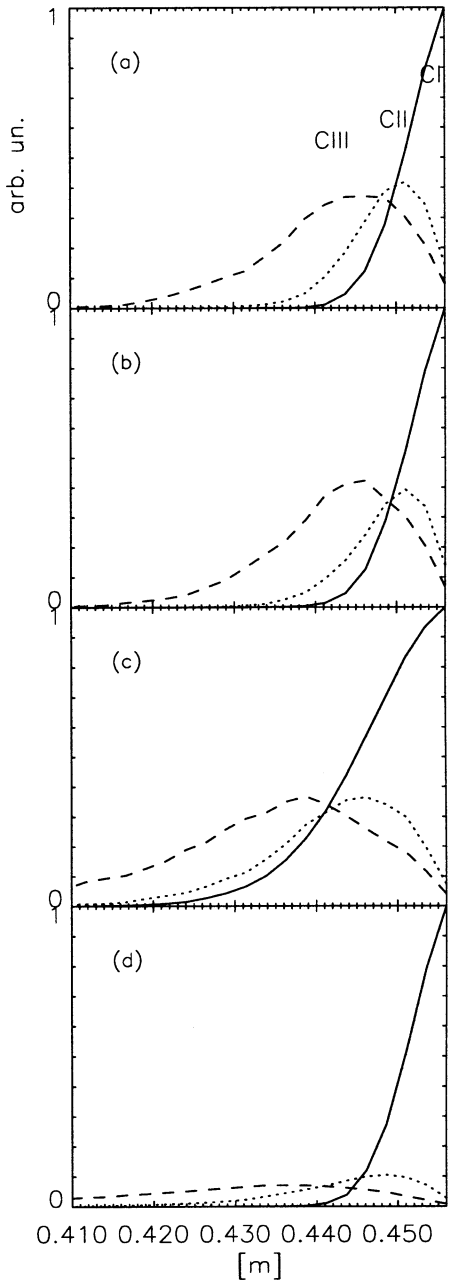

Figure 1. Radial profiles of lower ionization stages. CI, solid line; CII, short-dashed line; CIII, long-dashed line. The upper case shown refers to run 12 of Table 1. In the other column are shown: (a), run 1; (b) run 2; (c) run 5; (d) run 11. In abscissa is the radial coordinate; the wall is at 0.456 m.